Tellus (1996), 48A, 442–455
Printed in UK – all rights reserved

TELLUS
ISSN 0280-6495

The role of atmospheric waves in the laminated structure of ozone profiles at high latitude

By HECTOR TEITELBAUM[1]*, MOHAMED MOUSTAOUI[1], JOELLE OVARLEZ[1] and HENNIE KELDER[2], [1]*Laboratoire de Météorologie Dynamique du CNRS, Ecole Polytechnique, 91128 Palaiseau Cedex, France;* [2]*Royal Netherlands Meteorological Institute, Division of Geophysics, AE de Bilt, The Netherlands*

(Manuscript received 28 October 1994; in final form 2 October 1995)

ABSTRACT

A relationship between the laminated structure of ozone profiles and atmospheric waves has been found from some EASOE ozonesonde data. This result is derived first from the correlation of ozone and potential temperature fluctuations. Then, the analysis of simultaneous measurements shows that the same wave can explain the structure found at different sites. When the wind profile is available, it may be related to the ozone structure, confirming the role of waves in this phenomenon.

1. Introduction

The variations of ozone distribution under the influence of waves can be separated into two different types, regarding their scales: large-scale variations which become a subject of interest when satellite measurements show a relationship between ozone and temperature, and short-scale structure in vertical ozone profiles observed during ozonesonde ascent.

In this paper, we are interested in such short-scale, laminated ozone variations which are very often present in vertical profiles. They appear as alternative increases and decreases of the mixing ratio, at scales going from some hundreds of meters to several kilometres, with a duration of hours to days.

This paper is devoted to the analysis of such irregularities observed in the ozone profiles measured during the European Arctic Stratospheric Ozone Experiment (EASOE) which took place in the Arctic during the winter 1991–92 (Pyle et al. 1994).

* Corresponding author.

Dobson (1973) was the first to point out the existence of the laminated ozone structures observed during ozonesonde ascent. He noted also that well marked minima in the vertical distribution of ozone are found at heights of about 15 and 23 km. In an attempt to find the cause of these phenomena, Dobson studied the variation of their intensities, with both season and latitude. Ehhalt et al. (1983) noticed that the relative variances of long-lived trace gases show large differences which are greatly reduced when the local mean standard deviation is normalised to the local vertical mean gradient of the tracer's mixing ratio. They called this ratio "equivalent displacement height" (EDH), and showed that vertical profiles for all the long-lived trace gases are very similar when using this normalisation. This result demonstrates that variances are due to natural causes and not to measurement errors. Holton (1987) used the EDH and confirmed the hypothesis of Ehhalt et al. (1983). Furthermore, he noted the existence of two types of tracer variability: one highly correlated with potential temperature fluctuations, which can be attributed to vertical displacements of material surfaces induced by gravity waves; the other which is not associated with significant potential temperature oscillations, and could be produced by planetary scale waves. In this latter case, the absence of potential temperature oscillations could be due to the fact that parcel trajectories nearly coincide with the mean isentropes. Grudzev and Elanskiy (1984) used measurements of ozone variation obtained from an aircraft in a region of mountain waves as a good indicator of the characteristics of the waves. In some cases, they deduced the vertical displacement of air parcels from their measurements. After these experimental results, Gruzdev (1989) considered two mechanisms of variation of the total content of atmospheric trace gases in the presence of internal gravity waves: the deformation of the layer by vertical movements, and photochemical processes. He concluded that the layer deformation is mainly responsible for the variations of trace gases.

Very strong layering of ozone profiles were found by Deshler et al. (1990) on measurements made in Antarctica. They attributed the layering to exchange of air across the vortex edge. Similar results were obtained by Kyrö et al (1992) from the study of many ozone soundings made in the Arctic in 1989, but the layering was weaker than in the Antarctic. They explained this difference by the absence in Arctic of an ozone hole comparable to that in Antarctic. Furthermore, they found that the layering in ozone profiles is more pronounced outside and at the edge of the vortex than well inside it.

Following the studies of Dobson (1973), Reid et al. (1993) performed a statistical analysis of the laminated ozone distribution. They concluded that in January and February, the lamina arė present at all latitudes in a layer between 370–430 K potential temperature, but extending up to 550 K at high latitudes. They pointed out the association of these lamina with the polar vortex, and suggested that they could be induced in spring by the mixing of different air masses by synoptic-scale motions. Later on, Reid et al. (1994) confirmed from the analysis of the EASOE data, that the laminated ozone structures are more abundant near the vortex edge. They also examined a special case in which there exists a very strong irregularity in the ozone profile when an inertial gravity wave propagates in the region. The authors concluded that the wave appears too weak to be responsible for such strong irregularity, at least in this case, but they admit the possibility that waves may contribute to the formation of laminated ozone structures. In fact, from a study of ozone and water vapour vertical profiles measured during EASOE, Teitelbaum et al. (1994) (hereafter called TOKL) concluded that waves are able to produce the laminated structure in profiles of both minor constituents. In the present paper, by studying thoroughly the EASOE data, we shall show that waves play an important role in the ozone profiles lamination.

In Section 2, we present a model to explain the relation between the structure of ozone and potential temperature perturbations, and waves. In Section 3 we study examples which show good correlation between ozone and potential temperature fluctuations. We investigate further a case already presented in TOKL because it shows a very typical laminated structure, generated by a mountain wave. The comparison of simultaneous measurements carried out at different sites in Section 4, confirms that waves are the main mechanism inducing this type of irregularities in ozone profiles. Summary and conclusions are given in Section 5.

2. Relationship between laminated structure of ozone profiles and atmospheric waves

We consider that there are no source nor sink of ozone on the time scales relevant to the transport by gravity waves. In the Arctic, this is justified because the photochemical lifetime of ozone in the stratosphere below 25 km is very long, more than a year. This is due to the fact that ozone production mechanism as well as loss mechanisms depend on solar radiation, which is very weak in the winter Arctic lower stratosphere. Furthermore, as stated by Hartmann and Garcia (1979), Rood and Douglas (1985), and Douglas et al. (1985), the ozone perturbations induced by waves are independent of photochemical processes below 40 km. Then, in the absence of polar stratospheric clouds creating the possibility of rapid chemical destruction, laminated structure in the ozone profiles can be attributed to dynamical mechanisms.

To study the influence of waves in the formation of irregularities in ozone as well as in potential temperature distributions, it is useful to separate all the parameters into a mean and a perturbation:

$$f=\bar{f}+f'. \tag{1}$$

Here the mean is not as usually a zonal or temporal mean but the large scale filtered vertical profile.

In an inviscid fluid without source or sink of heat, the linearised equation for the potential temperature perturbation under the influence of a gravity wave writes

$$\mathrm{D}_t\,\theta'+\boldsymbol{u}'\cdot\nabla\bar{\theta}=0, \tag{2}$$

where θ is the potential temperature and

$$\mathrm{D}_t=\frac{\partial}{\partial t}+\bar{u}\,\frac{\partial}{\partial x}+\bar{v}\,\frac{\partial}{\partial y}. \tag{3}$$

The wave fields and the perturbations of minor constituent are represented as usually in complex form. The potential temperature fluctuation for instance writes as

$$\theta'=\theta'\,(z)\exp(i(\sigma t-k_x x-k_y y)), \tag{4}$$

where k_x and k_y are horizontal wave numbers, and σ is the frequency of the wave. Using (2) and taking into account (4), the potential temperature fluctuation normalised with respect to the mean can be written as

$$\frac{\theta'}{\bar{\theta}}=\mathrm{real}\left[\frac{i}{\Omega\bar{\theta}}\left(\frac{\partial\bar{\theta}}{\partial z}\,w'+\frac{\partial\bar{\theta}}{\partial x}\,u'+\frac{\partial\bar{\theta}}{\partial y}\,v'\right)\right], \tag{5}$$

where

$$\Omega=\sigma-k_x\bar{\mathrm{u}}-k_y\bar{\mathrm{v}}.$$

The perturbations of volume mixing ratio of a long-lived minor constituent, like ozone, is expressed in a very similar form. Indeed the conserved quantity in a fluid parcel following the flow is the volume mixing ratio. Its normalised fluctuation can be expressed as:

$$\frac{\chi'}{\bar{\chi}}=\mathrm{real}\left[\frac{i}{\Omega\bar{\chi}}\left(\frac{\partial\bar{\chi}}{\partial z}\,w'+\frac{\partial\bar{\chi}}{\partial x}\,u'+\frac{\partial\bar{\chi}}{\partial y}\,v'\right)\right]. \tag{6}$$

The expressions (5) and (6) have the same structure.

In some observations, the wind and ozone partial pressure hare been measured simultaneously. Thus, it is useful to use another equation for the perturbation.

Let us suppose, for simplicity, that the mean wind is zonal. Following Andrews and McIntyre (1978), and Plumb (1979), the perturbation of the conserved quantity can be written as

$$\chi'=-\xi'\cdot\nabla\bar{\chi}, \tag{7}$$

where ξ' is the Lagrangian perturbation associated with the particle displacement vector, whose components in the x, y and z directions are defined as:

$$\mathrm{D}_t\xi'=u^{\mathrm{l}}=u'+\zeta'\,\frac{\mathrm{d}\bar{u}}{\mathrm{d}z},\ \mathrm{D}_t\eta'=v',\ \mathrm{D}_t\zeta'=w', \tag{8}$$

respectively.

Expression (7) shows that if the gradient of the minor constituent is normal to the parcel trajectories there are no perturbations in the mixing ratio. Parcel trajectories are nearly ellipses which degenerate into straight lines for high frequency waves. They tilt with respect to the horizontal with an angle which decreases with the wave frequency. That means that the mixing ratio perturbations depend also on the type of wave producing them. Mountain waves, which probably occur very often in the Arctic region, produce an important vertical displacement of fluid particles. As shown by Lott and Teitelbaum (1993), these waves can propagate through the stratosphere when they are generated by a transient wind. The case of inertia-gravity waves, which have frequencies near the Coriolis frequency, is different in that the particle displacement is almost horizontal. It must be added that, even in this case, the fluid particles do not necessary follow an isentropic surface which can tilt with respect to the horizontal. Pure internal waves for which the Coriolis effect can be neglected are intermediate cases.

The correlation between the ozone and potential temperature perturbations will be very high if both gradients are parallel. As we study vertical profiles, we do not know horizontal gradients. Nevertheless, if ozone and potential temperature are nearly vertically stratified, we see from (6) or (7) that the relation between their perturbations can be easily calculated taking into account the mean vertical profiles. In fact both perturbations must be almost the same after multiplication of the potential temperature variation by the z-dependent coefficient:

$$R(z)=\left(\frac{1}{\bar{O}_3}\,\frac{\mathrm{d}\bar{O}_3}{\mathrm{d}z}\right)\left(\frac{1}{\bar{\theta}}\,\frac{\mathrm{d}\bar{\theta}}{\mathrm{d}z}\right)^{-1}. \tag{9}$$

The use of this factor is equivalent to the use of the EDH proposed by Ehhalt et al. (1983). The similarity of both perturbations is achieved with the use of this factor when ozone and potential temperature have the same horizontal gradient. Unfortunately, this is not always the case, especially when measurements hare made near the vortex edge, where the horizontal gradient of ozone can be very strong, leading to very large perturbations, even for small displacements of particles. It must be taken into account that, the vortex can be permeable to material parcels of fluid for small scale waves as suggested by McIntyre (1989). This means that irreversible transport can take place.

3. Correlation between ozone and potential temperature fluctuations

During the EASOE campaign some hundreds of ozonesonde balloons were launched from different sites at high latitude in the Northern Hemisphere. For some of them, temperature, pressure, altitude, and the wind (amplitude and direction) ware also measured in addition to ozone.

In Table 1, we give the name of the sites used in this study, together with their geographical co-ordinates. The map shows the position of these sites. Basically, the data processing of ozone and temperature profiles involves two main steps. The first is the use of a cubic spline to have equally spaced points in the vertical, say 40 m. Next, we use a low pass frequency filter to eliminate all fluctuations smaller than 6 km. The result is what we call a smoothed or basic state profile. Subsequently, another frequency band pass filter

Table 1. *Geographical coordinates of the launching sites used in this study*

Launching Site	Long. °E	Lat. °N
Egedesminde	−52.90	68.70
Lerwick	−1.18	60.13
Ny-Ålesund	11.95	78.93
Reykjavik	−22.60	63.97
Scoresbysund	−22.00	70.50
Sodankylä	26.60	67.40

which spans the range from 400 m to 6 km is used on the difference between the original and the basic state profiles. The last result is normalised with respect to the basic state and is what we name normalised perturbations. Other range of band pass filter are used in some cases to isolate particular wavelengths. The filter used is a non-recursive, low pass, ideal one. To avoid the Gibbs phenomenon we use a Kaiser window (R. W. Hamming, 1983)

We shall first analyse an ozone profile obtained on 11 December 1991. The launching site was Sodankylä and the launching time 11.35 U.T. The same day, Godin et al.(1994) found that a mountain wave appears as a trace on a polar stratospheric cloud (PSC) at 21 km altitude, extending 300 km east and west from Kiruna (21° E, 67.89° N). The PSC itself, being induced by the mountain wave. This profile was already presented in TOKL, but now we shall go deeply in the analysis of that mountain wave. Fig. 1 displays the vertical profile of ozone partial pressure and the wind blowing toward the S-E direction. The ozone profile shows some irregularities superim-

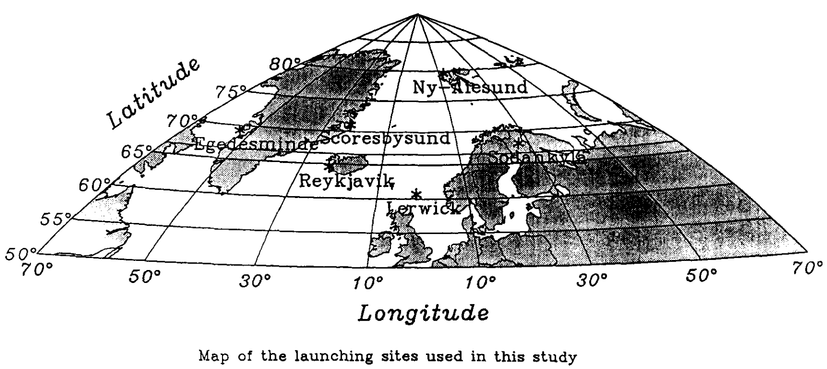

Map of the launching sites used in this study

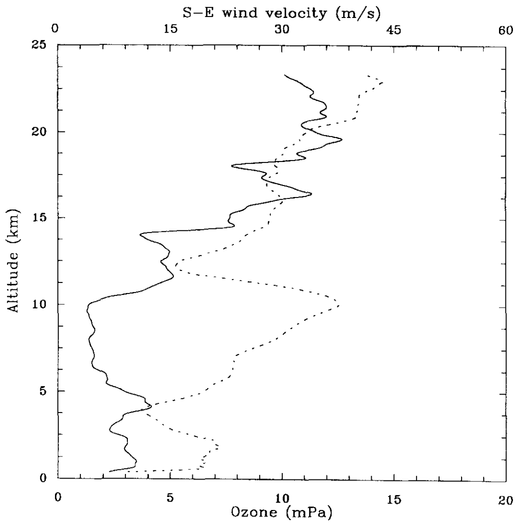

Fig. 1. Vertical profile of ozone partial pressure (solid line) and wind blowing in the S-E direction (dotted line), measured on 11 December 1991 at 11.35 UTC by a ozonesonde launched from Sodankylä.

posed to a typical profile. Similar irregularities are also observed in the wind profile. The reason for the wind direction will be explained below. The spectra of ozone, potential temperature, and wind in the S–E direction are shown in Fig. 2. All spectra show peaks near 4 km. In the light of these result, all profiles are filtered with a narrow band-pass filter (between 3 km and 5 km). Fig. 3a displays the wind perturbations projected on N-E and S-E axis. The amplitude of the S-E projection compared to the other shows that the wave is

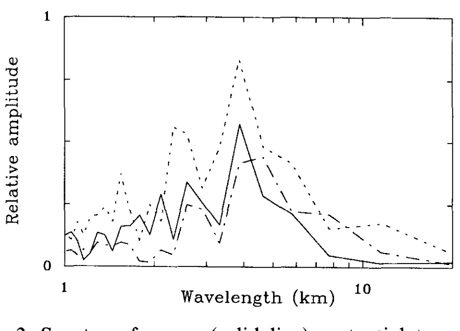

Fig. 2. Spectra of ozone (solid line), potential temperature (dotted line) and the wind component blowing in the S-E direction (dashed-dotted line). The data used are the same as for Fig. 1. All the spectra show peaks near 4 km.

linearly polarised in this direction. That is why we used these axis. The ozone and potential temperature perturbations after using the $R(z)$ factor are represented in Fig. 3b. The correlation is as high as 0.82. Coming back to Fig. 1 we can see that the wind component blowing toward the S-E has an amplitude around 30 m/s above 6 km and larger than 15 m/s near the ground. This is not very different from the wind measured at Bodo (14.4° E, 67.3° N) (see Godin et al. 1994), which is on the mountains. Those mountains probably generate the observed wave. Furthermore, as found by Ovarlez and Ovarlez (1994), the temperature near 20 km altitude, where the PSC was observed, reached the threshold temperature for NAT formation. This low value is due to the presence of the wave itself. This is in agreement with the relationship between mountain waves and PSC's formation found by Cariolle et al. (1989).

The horizontal wavelength of the wave, as determined by its trace on the PSC is approximately 40 km (Godin et al. 1994). Knowing the mean wind amplitude (30 m/s) we can calculate the vertical wavelength of the wave by a dispersion relation which writes as

$$k_z = \left[\frac{N^2 k_x^2}{(\sigma - k_x \bar{u})^2} - k_x^2 \right]^{1/2} \tag{10}$$

in the Boussinesq approximation.

Assuming a stationary or very long period wave (with respect to the ground, i.e., $\sigma = 0$), we find a vertical wavelength of approximately 11 km The phase of a mountain wave tilts downward in the direction of the mean wind. Moreover, the sounding balloon is transported horizontally by this wind and has an ascending velocity of 6 m/s. An elementary geometrical calculation shows that the balloon must have encountered two equivalent phase surfaces after a vertical displacement of 4 km which corresponds to the peak found in the spectra. In Fig. 4, an orographic map of the region is shown, together with the wind field obtained from the ECMWF analysis data on the same day. It is clearly seen that the wind blowing toward Sodankylä is highly dragged by the mountains. These are very favourable conditions for the generation of the mountain wave observed over Sodankylä.

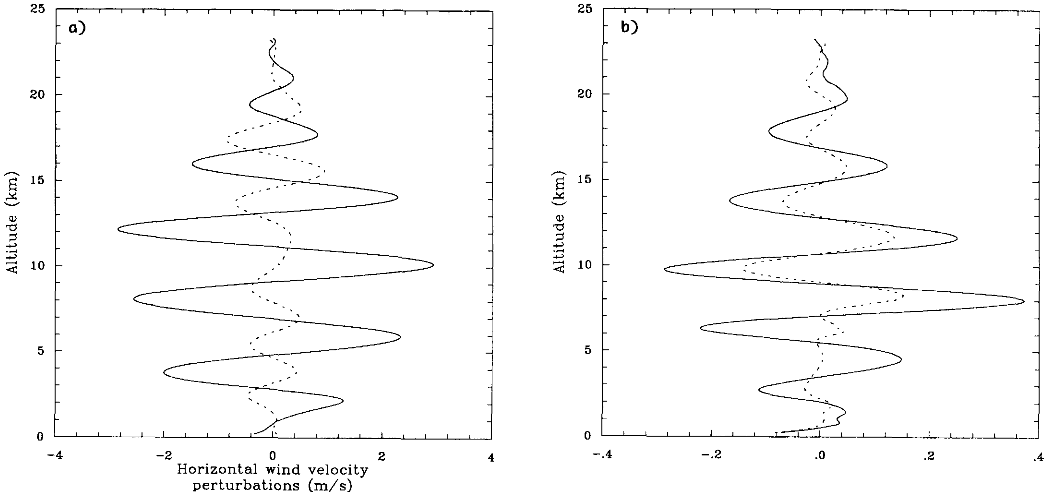

Fig. 3. Profiles for the measurements whose spectrum are shown in Fig. 2, but after using a band pass filter between 3 km and 5 km. (a) Wind components blowing in the S-E direction (solid line) and in the N-E direction (dotted line); (b) normalised fluctuations of ozone mixing ratio (solid line), and potential temperature (dotted line). The potential temperature fluctuations have been multiplied by the $R(z)$ factor.

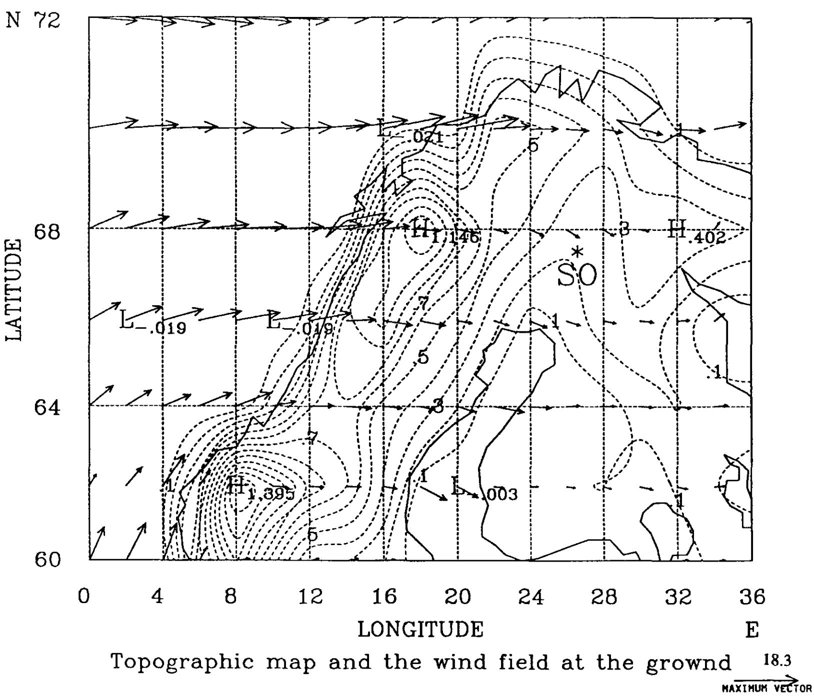

Fig. 4. Orographic map (contours are labelled in km), and horizontal wind field at the ground on 11 December 1991 at 12 UTC. The data are from ECMWF analysis. It is clearly seen that the wind blowing towards Sodankylä (SO) is highly dragged by the mountains.

In general, ozone, potential temperature, and even wind profiles are very irregular, and it is very difficult to distinguish whether there are one or many waves present.

We shall analyse an example in which it has been possible to separate two waves of different types and their effects on ozone and potential temperature. The launching site was also Sodankylä and the time of launching 9 December 1991 at 11.30 hr. Fig. 5 shows the ozone partial pressure and the eastward wind component. Both profiles exhibit an irregular vertical structure. After applying a band-pass filter which spans the range between 400 m and 12 km, the normalised ozone and potential temperature fluctuations have been plotted in Fig. 6. The potential temperature fluctuations have been multiplied by the $R(z)$ factor. It can be seen that there are similar irregularities of different thickness in both profiles. The correlation coefficient is 0.76. Notice that the largest fluctuations of normalised ozone mixing ratio are fairly often found near the tropopause. This characteristic is easily explained by the fact that the mean ozone mixing ratio varies abruptly in this region. The same explanation can be applied to potential temperature fluctuations.

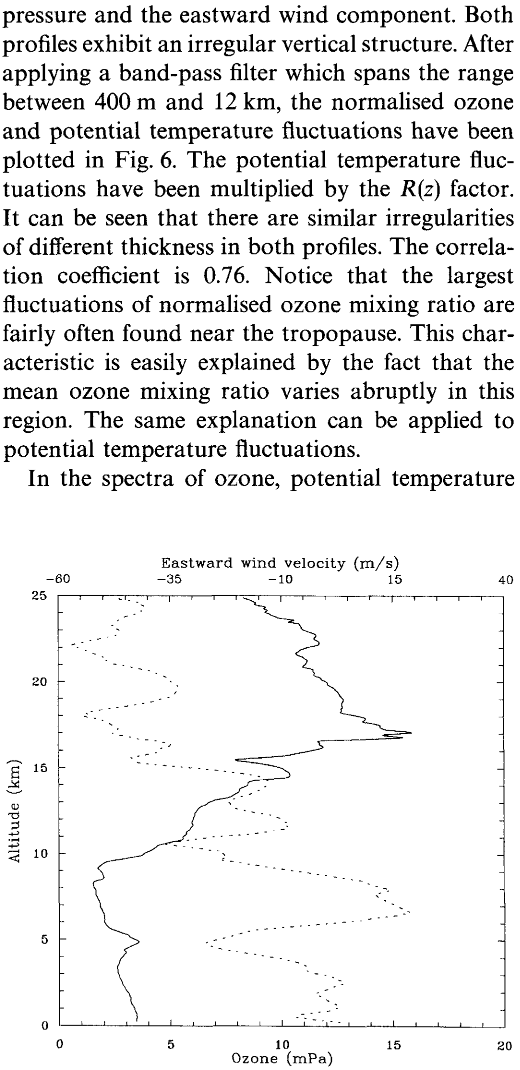

Fig. 5. Vertical profile of ozone partial pressure (solid line) and eastward wind (dotted line), measured on 9 December 1991 at 11.30 UTC, with a ozonesonde launched from Sodankylä.

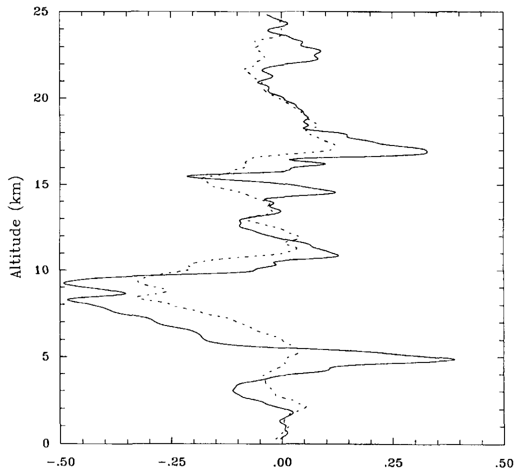

Fig. 6. Normalised fluctuations of ozone mixing ratio (solid line) and potential temperature (dotted line) corresponding to the same measurements as for Fig. 5. Potential temperature fluctuations have been multiplied by the $R(z)$ factor. The filter used spans a range between 400 m. and 12 km. This large band pass filter is used to distinguish two waves of different wavelengths.

In the spectra of ozone, potential temperature and zonal wind plotted in Fig. 7, there are two peaks at 3 km and 6 km. These two peaks suggest the existence of two different waves. To confirm this hypothesis, two band-pass filters have been used, one between 5 km and 7 km and the other between 2 km and 4 km. Fig. 8 displays the northward and eastward wind perturbations. The shorter wavelength perturbation is plotted on Fig. 8a.The two wind components are a quarter of cycle out of phase and have comparable amplitudes indicating the presence of a long period wave, probably an inertial gravity wave. The

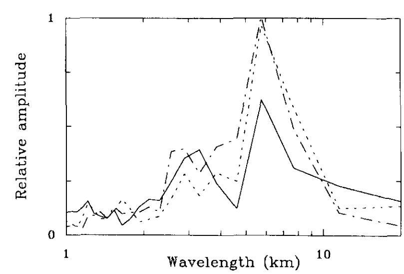

Fig. 7. Spectra of ozone (solid line), potential temperature (dotted line) and eastward wind (dashed-dotted line) corresponding to the same measurements as for Fig. 5. There are two peaks at 3 km and 6 km.

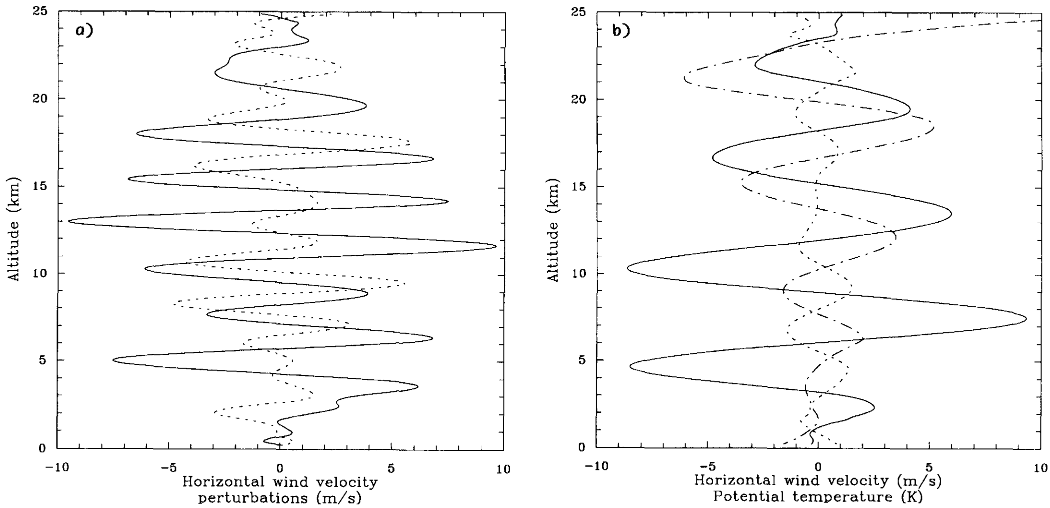

Fig. 8. Eastward (solid line) and northward (dotted line) wind perturbations corresponding to the same measurements as in Figs. 5, 6, and 7. (a) After using a filter which spans the range between 2 km and 4 km. The two wind components are a quarter of cycle out of phase, and of comparable amplitude, indicating a long period wave, probably an inertial gravity wave. (b) After using a filter which spans the range between 5 km and 7 km. The main wind oscillation is zonal indicating a short period wave. For the wave of this wavelength the potential temperature has been plotted too (dashed-dotted line). The potential temperature and the zonal wind are a quarter of cycle out of phase. (The significance of this phase difference is given in the text).

longer wavelength perturbation is plotted in Fig. 8b. The main wind oscillation is practically zonal (i.e. linearly polarised) indicating the presence of a short period wave. For this wavelength wave the potential temperature has been also plotted in this figure. The potential temperature and the zonal wind are a quarter of cycle out of phase. This result can be interpreted in the following way: in the mean wind system, the particle displacements are maximum where the wave induced wind velocity vanishes. Consequently, the potential temperature perturbation must be maximum at this level.

We shall now show that the vertical gradient of the basic state plays an important role in the ozone-potential temperature correlation. Fig. 9 concerns the result obtained on 8 February 1992, at Sodankylä. Fig. 9a displays the ozone partial pressure profile. The laminated structure is present superimposed to a typical profile. The ozone and potential temperature spectra plotted in Figure 9b show a common peak between 8 km and 9 km. Even if this latter wavelength is large with respect to the sample length, it will be considered because it is very marked in both profiles. Fig. 10 shows ozone and potential temperature fluctuations after using two different band-pass filters. The 8.5 km wavelength perturbations are shown on Fig. 10a after using a band-pass filter between 5 km and 10 km Both profiles are very similar. Fig. 10b shows also ozone and potential temperature fluctuations after using a filter excluding the main peak (400 m to 5 km). The correlation coefficient is 0.68. In this case the potential temperature fluctuations without the $R(z)$ factor are also displayed. The present analysis proves that the particle displacements which generate the laminated ozone structure do not take place on isentropic surfaces. This latter scenario should not give potential temperature fluctuations. Furthermore, the changes induced by the use of the $R(z)$ factor indicate that the vertical displacements induced by waves play a very important role.

Fig. 11 shows the results obtained on 3 December 1991, at Egedisminde. The spectra of ozone, potential temperature and zonal wind exhibit a common peak at 3.5 km (Fig. 11a). After using a filter which spans the range between 2.5 km and 4.5 km, the ozone and potential temperature fluctuations are plotted in Fig. 11b. The

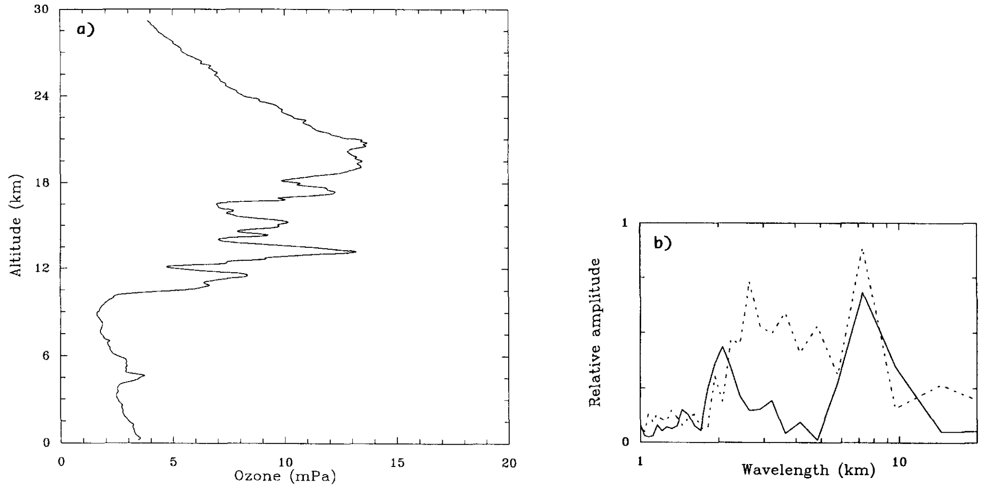

Fig. 9. Measurements corresponding to a radio sounding launched from Sodankylä on 8 February, 1992 . (a) Ozone partial pressure profile, (b) spectra of ozone (solid line) and potential temperature (dotted line) . A common peak is clearly seen at 8 km.

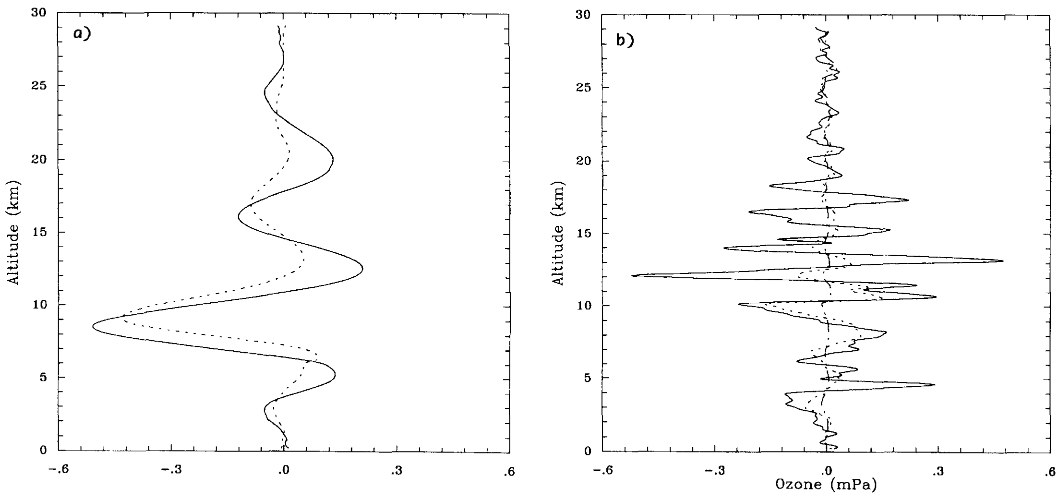

Fig. 10. Ozone and potential temperature fluctuations corresponding to the same measurements as for figure 9. (a) Ozone (solid line), and potential temperature fluctuations (dotted line) after using a filter which spans the range between 5 km and 10 km to show the oscillations corresponding to the 8 km peak. (b) Same as (a), but after using a filter which spans the range between 400 m and 5 km. The potential temperature is also plotted without using the $R(z)$ factor (dotted-dashed line).

correlation coefficient is very high: 0.91. Fig. 11c shows the eastward and northward wind fluctuations. The two wind components are a quarter of cycle out of phase and have practically the same amplitude, indicating the presence of a long period wave. The phase lag between both wind components shows that it is an upward propagating wave. The study of this case has been restricted to a layer between 4 km and 14 km where the coherence of the different profiles is the best. This choice is justified by the short vertical wavelength of the wave.

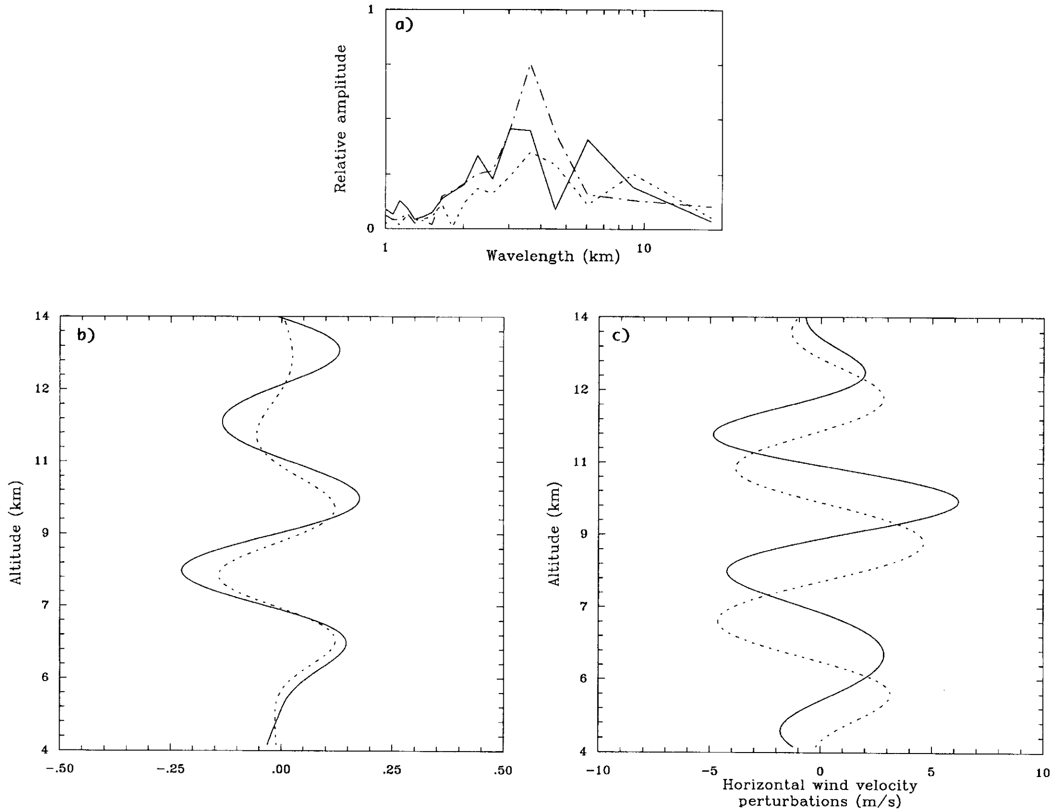

Fig. 11. Measurements corresponding to a radio sounding launched from Egedesminde on 3 December, 1991. (a) Spectra corresponding to ozone (solid line), potential temperature (dotted line) and zonal wind (dashed-dotted line). There is a common peak at 3.5 km. (b) Ozone (solid line) and potential temperature fluctuations (dotted line) after using a filter which spans the range between 2.5 km and 4.5 km. The $R(z)$ factor has been used. (c) Zonal (solid line) and meridional (dotted line) winds components after using the same filter as in (b).

As it has been already proved, the laminated structure of the ozone profile can be the effect of more than one wave. We shall show two cases for which we used a large band-pass filter which spans the range between 2 km and 10 km. Fig. 12 corresponds to measurements performed on 29 December 1991, at Sodankylä. This figure shows the ozone perturbations and the potential temperature perturbation with and without the $R(z)$ factor. Again the role of this factor is clearly seen. The value of the correlation coefficient is 0.74. A similar case is shown in Fig. 13. It corresponds to measurements performed on 7 December 1991, at Ny-Ålesund. The amplitude of the potential temperature fluctuations agree well to that of the ozone after the use of the $R(z)$ factor. The value of the correlation coefficient is 0.82.

The analysis of the data carried out in this section shows several arguments favouring the interpretation of the ozone laminated structures as being produced by waves. One is the existence of alternate increases and decreases of ozone of nearly the same thickness around a smoothed vertical profile, giving well defined and significant peaks in the spectra. Other is the similarity observed in the structure of the irregularities in ozone mixing ratio and potential temperature profiles. Finally when wind measurements are available it show the signature of the same wave in ozone and in potential temperature.

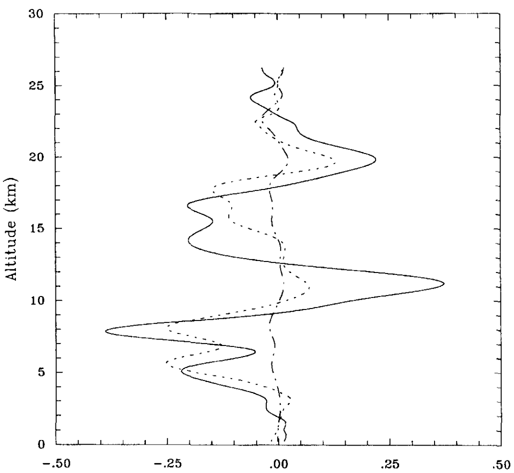

Fig. 12. Ozone fluctuations (solid line) and potential temperature fluctuations using the $R(z)$ factor (dotted line) and without this factor (dashed-dotted line). The measurements correspond to a radio sounding launched from Sodankylä on 29 December, 1991. A large band pass filter which spans the range between 2 km and 10 km has been used.

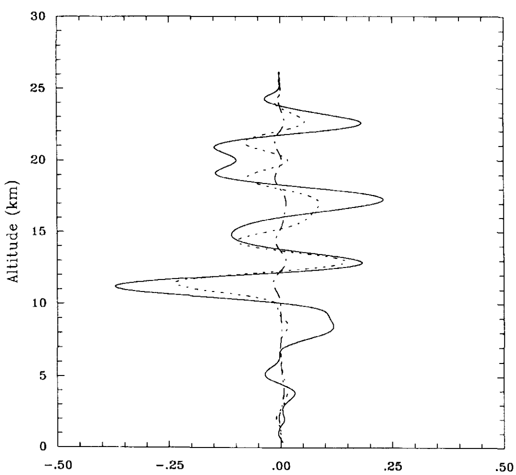

Fig. 13. Ozone (solid line) and potential temperature fluctuations using the $R(z)$ factor (dotted line) and without this factor (dashed-dotted line).The filter used spans a range between 2 km and 10 km. The measurements correspond to a radio sounding launched from Ny-Ålesund on 7 December, 1991.

Furthermore in some cases, it is possible to determine the type of wave involved.

Now we shall compare simultaneous measurements performed at different sites to give more arguments in favour of the hypothesis of wave induced laminated structure.

4. Comparison of simultaneous measurements

In this section we shall study some characteristics of simultaneous measurements performed on different sites to confirm the wave hypothesis. If the same wave propagates over two or more launching stations, we can observe structures having the same vertical wavelength. Nevertheless the phases as a function of altitude or potential temperature can be different. These phase differences, particularly as a function of potential temperature, are a signature of the wave and weaken the hypothesis of sliding of isentropic layers.

On 13 December 1991, twelve ozonesondes were launched from 12 different sites. We shall analyse three of them because they were simultaneous. The launching sites were: Egedesminde, Lerwik and Reykjavik. The first step is to compare the spectra of ozone for the three sites. This part of the analysis deserves some comments. As explained above, if a profile exhibits an oscillatory structure, the vertical wavelength seen by the balloon depends on the tilt of the phase surfaces with respect to the balloon trajectory. Consequently the apparent wavelength can be different on different sites. Nevertheless, we can admit that if the same wave propagates above different sites, the phase surfaces must tilt with the same angle. Furthermore, if the mean horizontal wind is approximately the same, the balloon must see approximately the same vertical wavelength. Fig. 14 shows the results obtained over these three stations. The spectra corresponding to Egedesminde and Reykjavik present a peak at 7 km (Fig. 14a). Even if this peak is not apparent at Lerwik there is an increase between 5 km and 10 km. Fig. 14b shows the three ozone profiles as a function of potential temperature, after the use of a band-pass filter between 5 km and 9 km. There is a phase shift between the profiles, the one corresponding to Reykjavik having an intermediate position with respect to the others. It can be remarked that Reykjavik is placed in an intermediate geographic position between the other two stations. This result strongly suggests the presence of a single wave responsible on the particular vertical structure above the three sites.

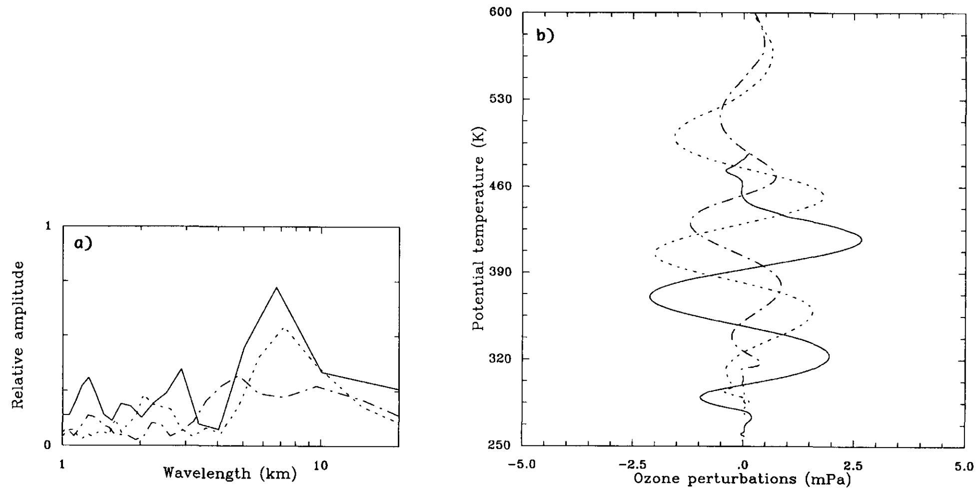

Fig. 14. Simultaneous measurements corresponding to radio soundings launched from three different sites: Egedismende, Lerwick and Reykjavik on December 13, 1991. (a) Spectra of ozone from Egedismende (solid line), Lerwick (dashed-dotted line) and Reykjavik (dotted line). The Egedismende and Reykjavik spectra present a peak around 7 km. (b) Ozone profiles as a function of potential temperature after using a filter which spans the range between 5 km and 9 km.

As explained above, due to the horizontal displacement of the balloon, we cannot go further in the analysis of the wave characteristics: the 7 km vertical wavelength is an apparent one.

Finally, we shall analyse three other soundings performed on 11 December 1991. The launching stations where Reykjavik, Scoresbysund and Ny-Alesund. The first two were simultaneous whereas the last occurs one hour before. It must be remarked that the first case we analysed and in which we attributed the ozone and potential temperature fluctuations to a mountain wave, corresponds to measurements performed the same day. Nevertheless, the three sites mentioned above are in a very different region: they are separated from Sodankylä by a chain of mountains as can be seen on the map. The spectra of the ozone profiles displayed in Fig. 15a show a well defined peak near 6 km at the three sites. After a filtering process which spans the range between 4 km and 8 km, the three profiles are presented in Fig. 15b, as functions of altitude. As in the previous example, we note a phase shift between the three stations, with an intermediate position for the Scoresbysund profile. This intermediate position is also geographical. The same profiles are plotted in Fig. 15c, but as functions of potential temperature. The shift of the phases is ordered as in the altitude representation.

5. Summary and conclusion

During de EASOE campaign, many ozonesondes were launched from different sites in the Northern Hemisphere. Most of the sites were situated at high latitudes in the Arctic. Simultaneous measurements of temperature, pressure, ozone and sometimes of wind were performed. The measured ozone profiles often exhibit alternative increases and decreases of the mixing ratio with respect to a smoothed vertical profile. We studied some of these measurements to determine the role of propagating waves in the formation of the laminated ozone structure. In the first part of our analysis, we compare ozone and potential temperature fluctuations for individual soundings. The correlation between the vertical fluctuations of ozone and potential temperature is very good after the use of a vertical dependent factor similar to the EDF used by Ehhalt et al.(1983), and Holton (1987). A mountain wave identified by Godin et al. (1994) as a trace over a PSC has been proved to be the cause of the ozone

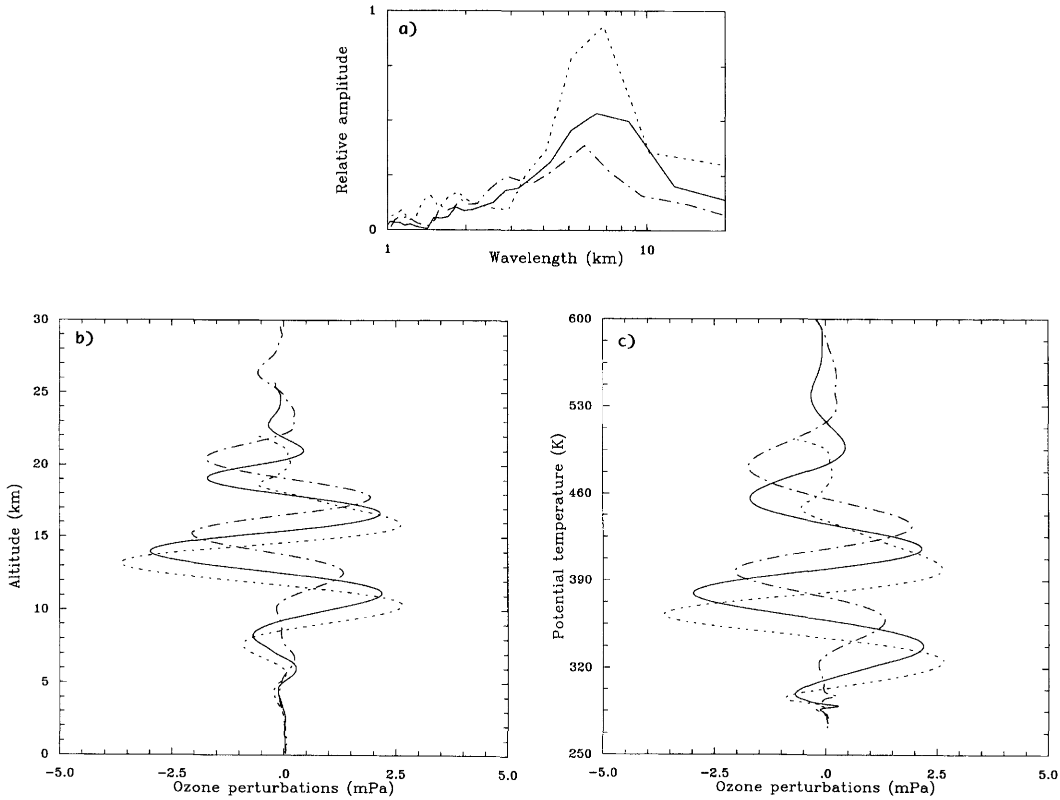

Fig. 15. Simultaneous measurements corresponding to radio soundings launched from three different sites: Scoresbysund, Ny-Ålesund and Reykjavik on 11 December, 1991. (a) Spectra of ozone from Scoresbysund (solid line), Reykjavik (dashed-dotted line) and Ny-Ålesund (dotted line). All the three spectra show a peak between 6 and 7 km. (b) Ozone profiles as a function of altitude after using a filter which spans the range between 4 km and 8 km. (c) The same as in (b) but as a function of potential temperature.

and potential temperature laminated structure. In general there is more than a wave propagating simultaneously, rendering the interpretation more difficult. Nevertheless it has been possible to identify the trace of two waves in the ozone, potential temperature and wind profiles for particular sounding. Some characteristics of the waves found in the wind profile suggest that there are waves of two different types. One is polarised in a plane, and is probably a mountain wave. The other has a shorter wavelength, the two wind components being a quarter of cycle out of phase, what characterizes long period wave, probably an inertial gravity wave.

Simultaneous measurements at two or three different sites show in general, very similar structure in ozone. Moreover, the structure is shifted in altitude or potential temperature from one site to the other. The shift is ordered as the geographical position. This last characteristic clearly indicates that the structure is due to atmospheric waves.

We conclude that different types of waves play a very important role in the formation of the laminated structure of ozone. Especially those appearing as alternated increases and decreases of mixing ratio about a mean vertical profile. Nevertheless we can not exclude other mechanisms in the formation of more irregular variations.

6. Acknowledgements

We acknowledge the participants in the EASOE campaign who provided the data used in this analysis: R. Fabian, M. Gil, P. A. Hughes, T. S. Jorgensen, E. Kyro. The computations presented in this paper were funded by the "Institut du Développement et des Ressources en Informatique Scientifique".

REFERENCES

Andrews, D. G. and McIntyre, M. E. 1978. An exact theory of non-linear waves on a Lagrangian-mean flow. *J. Fluid Mech.* **89**, 609–646.

Cariolle, D., Muller, S., Cayla, F. and McCormick, M. P. 1989. Mountain waves, polar stratospheric clouds, and the ozone depletion over Antarctica. *J. Geophyis. Res.* **94**, 11233–11240.

Deshler, T., Hofmann, D. J. and Herefold, J. V. 1990. Ozone profile measurements within, at the edge of, and outside the Antarctic polar vortex in the spring of 1988. *J. Geophys. Res.* **95**, 10,023–10,035.

Dobson, G. M. B. 1973. The laminated structure of the ozone in the atmosphere. *Quart. J. R. Met. Soc.* **99**, 599–607.

Douglas, A. R., Rood, R. B. and Stolarski, R. S. 1985. Interpretation of ozone temperature correlations 2. Analysis of SBUV ozone data. *J. Geophys. Res.* **90**, 10,693–10,708.

Ehhalt, D. H., Röt, E. P. and Schmidt, U. 1983. On the temporal variance of stratospheric trace gas concentrations. *J. Atmos. Chem.* **1**, 27–51.

Godin, S., Megie, G., David, C., Haner, D., Flesia, C. and Emery, Y. 1994. Airborne lidar observation of mountain-wave-inducedpolar stratospheric clouds during EASOE. *Geophys. Res. Lett.* **21**, 1335–1338.

Gruzdev, A. N. and Elanskiy, N. F. 1984. Ozone observations in the region of mountain lee waves. *Izvestiya, Atmos. and Ocean. Phys.* **20**, 632–638.

Gruzdev, A. N. 1989. Mechanism of variations in total content of trace gases under the influence of internal gravity waves. *Izvestiya, Atmos. and Ocean. Phys.* **25**, 357–362.

Hamming, R. W. 1983. Digital filters. Englewood Cliffs:Prentice-Hall 257 pp.

Hartmann, D. L. and Garcia, J. 1979. A mechanistic model of ozone transport by planetary waves in the stratosphere. *J. Atmos. Sci.* **36**, 350–364.

Holton, J. R. 1987. The production of temporal variability in trace constituents concentrations. *In: Transport process in the middle atmosphere* (G. Visconti and R. Garcia, eds.). D. Reidel Publishing Company pp. 313–326.

Kyrö, E., Taalas, P., Jorgensen,T. S., Knudsen, B., Stordahl, F., Braathen, G., Dahlback, A., Neuber, R., Krüger, B. C., Dorokhov, V., Yuskov, V. A., Rudakov, V. V. and Torres, A. 1992. Analysis of the ozone soundings made during the first quarter of 1989 in the Arctic. *J. Geophys. Res.* **97**, 8083–8091.

Lott, F. and Teitelbaum, H. 1993. Linear unsteady mountain waves. *Tellus* **45A**, 201–220.

McIntyre, M. E. 1989. On the Antarctic ozone hole. *J. Atmos. Terr. Phys.* **51**, 29–43.

Ovarlez, J. and Ovarlez, H. 1994. Stratospheric water vapour content evolution during EASOE. *Geophys. Res. Lett.* **21**, 1235–1238.

Plumb, R. A. 1979. Eddy fluxes of conserved quantities by small-amplitude waves. *J. Atmos. Sci.* **36**, 1699–1704.

Pyle, J. A., Harris, N. R. P., Farman, J. C., Arnold,F., Braathen, G., Cox, R. A., Faucon, P., Jones, R. L., Megie, G., O'Neill, A., Platt, U., Pommereau, J. P., Schmidt, U. and Stordal,F. 1994. An overview of the EASOE campaign. *Geophys. Res. Lett.* **21**, 1191–1194.

Reid, S. J., Vaughan, G. and Kyro, E. 1993. Occurrence of ozone laminae near the boundary of the stratospheric polar vortex. *J. Geophys. Res.* **98**, 8883–8890.

Reid, S. J., Vaughan, G.,Mitchell, N. J., Prichard, I. T., Smit, H. J., Jorgensen, T. S., Varotsos, C. and de Backer, H. 1994. Distribution of ozone laminae during EASOE and the possible influence of inertia-gravity-waves. *Geophys. Res. Lett.* **21**, 1479–1482.

Rood, R. B. and Douglas, A. R. 1985. Interpretation of ozone temperature correlations. 1. Theory. *J. Geophys. Res.* **90**, 5733–5743.

Teitelbaum, H., Ovarlez, J., Kelder, H. and Lott, F. 1994. Some observations of gravity-wave-induced structure in ozone and water vapour during EASOE. *Geophys. Res. Lett.* **21**, 1483–1486.